ISSN 0020-1685, Inorganic Materials, 2018, Vol. 54, No. 1, pp. 96–101. © Pleiades Publishing, Ltd., 2018.
Original Russian Text © G.D. Nipan, 2018, published in Neorganicheskie Materialy, 2018, Vol. 54, No. 1, pp. 104–109.

Specific Phase Transformations of K/W/Mn/SiO_2 Composite Catalyst

G. D. Nipan

Kurnakov Institute of General and Inorganic Chemistry, Russian Academy of Sciences, Leninskii pr. 31, Moscow, 119991 Russia
e-mail: nipan@igic.ras.ru

Received June 26, 2017

Abstract—This paper analyzes results obtained in studies of K/W/Mn/SiO_2 composite catalysts for the oxidative coupling of methane (OCM) and examines phase transformations involving melts that form in the K_2O–WO_3–Mn_2O_3–SiO_2 system at typical temperatures of the heterogeneous OCM process.

Keywords: phase transformations, multicomponent systems, oxide composites, catalysts
DOI: 10.1134/S0020168518010119

INTRODUCTION

K/W/Mn/SiO_2 composites are effective catalysts for the oxidative coupling of methane (OCM). Along with Na/W/Mn/SiO_2 composites [1], they ensure high yields of C_{2+} products (ethylene, ethane, and heavier hydrocarbons) in the OCM, but little attention has so far been paid to the potassium-containing catalysts.

Without tungsten, the addition of K (or Cs) to a 10% Mn/SiO_2 catalyst did not increase the yield of C_{2+} products (Y_{C_2} = 8%) in the OCM (800°C, 2.0 L/(g h), CH_4 : air = 0.55 : 1) [2]. The low catalytic activity of a 2.7% K_2WO_4/SiO_2 composite (conversion X_{CH_4} = 1–2% and selectivity S_{C_2} = 33–35%) for the OCM (650°C, 2.82 L/h, CH_4 : O_2 = 9 : 1, continuous-flow quartz microreactor) probably resulted from the relatively low process temperature and the formation of the $K_2W_2O_7$ tungstate instead of K_2WO_4 (as suggested by Raman spectroscopy data) [3]. Samples with the overall composition K(Rb,Cs)$_2WO_4$/55SiO_2, prepared via impregnation of a silica support, contained a mixture of cristobalite and tridymite—crystalline SiO_2 polymorphs (no K, Rb, or Cs tungstate was detected experimentally). The C_2 yield in the OCM (850°C, 101 kPa, 1.08 L/h, CH_4 : O_2 : He = 4.5 : 1 : 44.5, continuous-flow alundum microreactor) was 20% for K (X_{CH_4} = 30%, S_{C_2} = 67%), 25% for Rb (X_{CH_4} = 32%, S_{C_2} = 78%), and 18% for Cs (X_{CH_4} = 33%, S_{C_2} = 55%) [4]. The addition of Mn increased Y_{C_2} to 26% (X_{CH_4} = 29%, S_{C_2} = 90%) for the K-containing composite and reduced Y_{C_2} to 19.5% (X_{CH_4} = 31%, S_{C_2} = 63%) for the Rb-containing composite [4]. However, after powder of the K-containing composite (2K/W/1.2Mn/55SiO_2) was applied to an Y_2O_3-stabilized ZrO_2 (YSZ) ceramic solid electrolyte, the Y_{C_2} yield did not exceed 10% (X_{CH_4} = 19%, S_{C_2} = 54%), no matter whether oxygen was electrochemically introduced into the OCM process (850°C, 3.6 L/h, CH_4 : O_2 : He = 9 : 1 : 27) or the gases were admitted together [5]. This result can be accounted for by the predominant weight of the YSZ ceramic, which is, per se, capable of ensuring Y_{C_2} near 11% in the OCM process [6]. A 5% K_2WO_4/2% Mn/SiO_2 sample prepared via impregnation made it possible to obtain stable Y_{C_2} at a level of 18.6% (X_{CH_4} = 29.8%) for continuous OCM (800°C, 101 kPa, 25.4 L/(g h), CH_4 : O_2 = 3.2 : 1, quartz microreactor). In addition to cristobalite and trace levels of tridymite and the Mn_2O_3 manganese oxide, it was found to contain K_2WO_4 [7]. Similar results for the OCM (800°C, 6.7 L/h, CH_4 : O_2 = 5 : 1, quartz reactor) were obtained with a 5% K_2WO_4/4% Mn/SiO_2 composite (Y_{C_2} = 20%, X_{CH_4} = 29%, S_{C_2} = 70%) [8]. Samples with the compositions 0.78% K/3.13% W/4% Mn/SiO_2 (Y_{C_2} = 23%, X_{CH_4} = 32%, S_{C_2} = 73%) and 0.1% K/3.13% W/4% Mn/SiO_2 (Y_{C_2} = 16%, X_{CH_4} = 26%, S_{C_2} = 63%) differed markedly in catalytic activity and, synthesized by the same method (impregnation), they contained hubnerite ($MnWO_4$) along with cristobalite, tridymite, Mn_2O_3, and K_2WO_4 [8]. Note that no cesium tungstates were detected in Cs/W/Mn/SiO_2 composites, but Y_{C_2} for various compositions was 18–19% [8]. The use of solid-state reaction for the preparation of a 2K/W/2Mn/91SiO_2 composite [9–11] allowed $Y_{C_{2+}}$ values near 27% (X_{CH_4} = 41%, $S_{C_{2+}}$ = 66%) to be reached in some cases in the OCM process (882°C, 101 kPa, 60–63 L/(g h), CH_4 : O_2 = 2.4 : 1, quartz reactor), but the presence of K_2WO_4 in the composite remained open to question [11]. For com-

parison, the highest $Y_{C_{2+}}$ values for 2Rb/W/2Mn/91SiO_2 and 2Cs/W/2Mn/91SiO_2 composites were 26% (X_{CH_4} = 42%, S_{C_2} = 61%) and 20% (X_{CH_4} = 40%, S_{C_2} = 52%) [11] and the composites were found to contain trace levels of tungstates. Thus, interaction of WO_4 tetrahedral and MnO_6 octahedral groups on the surface of a neutral SiO_2 support [12] cannot explain the OCM mechanism when the most efficient K/W/Mn/SiO_2 catalyst prepared by solid-state reaction is used.

The purpose of this work is to identify the nature of the phase transformations in a K/W/Mn/SiO_2 composite at typical OCM temperatures.

RESULTS AND DISCUSSION

According to X-ray diffraction data (Fig. 1), the catalytically effective composite 2K/W/2Mn/91SiO_2 prepared by solid-state reaction contained cristobalite and trace levels of tridymite, bixbyite (Mn_2O_3), and an unidentified phase (or phases) [11], presumably similar to cryptomelane, KMn_8O_{16} [13]. The phase composition of the 2K/W/2Mn/91SiO_2 composite is essentially identical to that of a 2% KMnO4/SiO_2 catalytically inert composite (Fig. 1, scan *3*) (Rigaku Miniflex 600, CuK_α radiation, λ = 1.541 Å; sample prepared at a pressure of 2.5 GPa and temperature of 500°C [14]). Moreover, not only are the mixed oxides $KMnO_4$, K_2MnO_4, and K_3MnO_4 [15] unfavorable for the OCM process, but they also oxidize the forming ethylene [16].

Thus, the presence of crystalline phases of the K–Mn–O system and SiO_2 polymorphs in a composite does not ensure catalytic activity of K/W/Mn/SiO_2 for the OCM process. After solid-state synthesis of the composite, no potassium tungstates were detected experimentally (Fig. 1). Therefore, the catalytic activity of K/W/Mn/SiO_2 is unrelated to metastable tungstates [17] or tungsten bronzes [18] in the K_2O–WO_3 system. Even in the case of the formation of alkali tungstates, their concentration in the composites decreases during heat treatment on account of volatility, which increases in going from Li to Cs [19]. In vacuum, sublimation or vaporization occurs congruently owing to the predominant formation of M_2WO_4 molecules in vapor [19]. In air, the process is incongruent because, in addition to M_2WO_4 molecules, there are M_2O molecules [20] and, in the presence of reductants, M atoms [21]. In the condensed phase, the initial M : W ratio changes and, even though the melting points of phase-pure M_2WO_4 (M = K, Rb, Cs) exceed 900°C, the forming mixtures of K, Rb, and Cs polytungstates [20] melt eutectically at typical OCM temperatures [17] and lose the alkali element during the OCM to the extent of converting into WO_3, which can sublime congruently [21]. Finally, in the course of prolonged OCM, the alkali tungstates disappear from Li(Na,K,Rb,Cs)/W/Mn/SiO_2 composites [1].

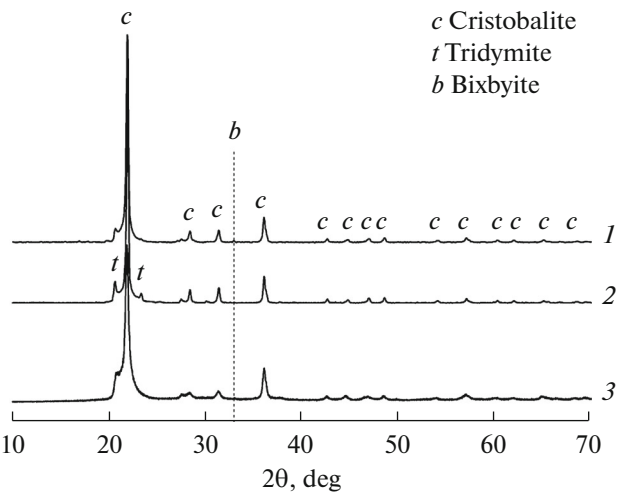

Fig. 1. X-ray diffraction patterns of the (*1*, *2*) K/W/Mn/SiO_2 (before and after OCM, respectively) and (*3*) K/Mn/SiO_2 composites.

The active catalytic component of the Li(Na,K,Rb,Cs)/W/Mn/SiO_2 composites is a melt, which favors cristobalite recrystallization into tridymite and quartz [22, 23]. That the alkali metal oxides differ in their solubility in the SiO_2 polymorphs leads to the diffusion of alkali cations and, accordingly, the diffusion of oxygen anions, which determine its activity for the OCM [22, 23]. This is indirectly supported by the catalytic inertness of Mg(Ca,Sr,Ba)/W/Mn/SiO_2 composites [4, 7], because no melts are formed at typical OCM temperatures in systems containing alkaline metal oxides.

In the case of Li(Na)/W/Mn/SiO_2, the components that melt are the starting tungstates $Li(Na)_2WO_4$ [24, 25], but in the case of K(Rb,Cs)/W/Mn/SiO_2 this is not so and the phase picture is more complex.

For comparison, Fig. 2a represents a model for the subsolidus phase equilibria in the pseudoquaternary system K_2O–WO_3–Mn_2O_3–SiO_2 at a constant temperature of 600°C and an oxygen partial pressure of 20 kPa. The representative points indicate the compositions of the crystalline phases in an idealized K_2O–WO_3–Mn_2O_3–SiO_2 system. Tungstates, silicates, and manganates are represented by the first letters in the symbols of their constituent cations and the subscripts: K_4W, K_6W_2, K_2W, K_2W_2, K_2W_3, K_2W_4, and K_2W_6 correspond to K_4WO_5, $K_6W_2O_9$, K_2WO_4, $K_2W_2O_7$, $K_2W_3O_{10}$, $K_2W_4O_{13}$, and $K_2W_6O_{19}$; K_2S , K_2S_2, and K_2S_4 correspond to K_2SiO_3 , $K_2Si_2O_5$, and $K_2Si_4O_9$. The K_3M, K_2M_4, and K_2M_8 squares represent nonstoichiometric phases based on K_3MnO_4 [15, 26], $K_2Mn_4O_8$ [26–29], and $K_2Mn_8O_{16}$ [27–29], which formally do not belong to the K_2O–Mn_2O_3 system, but can exist at the temperature and oxygen partial

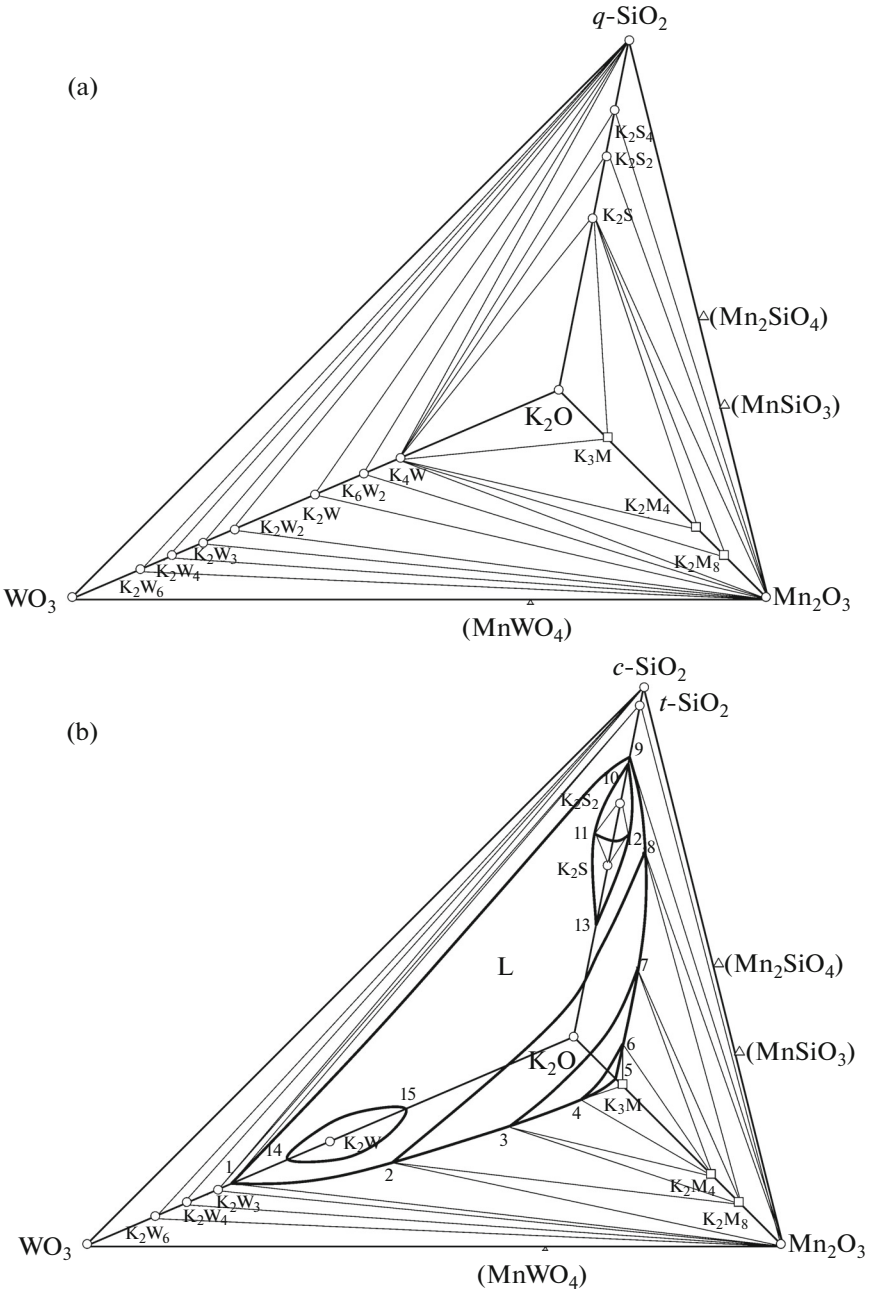

Fig. 2. Isobaric–isothermal phase diagrams of the K_2O–WO_3–Mn_2O_3–SiO_2 system: (a) $t = 600°C$, $p_{O_2} = 20$ kPa; (b) $t = 800°C$, $p_{O_2} = 20$ kPa (q-SiO_2 = quartz).

pressure chosen. In this paper, phase equilibria involving $MnSiO_3$, Mn_2SiO_4, and $MnWO_4$ (represented by triangles); the compounds $K_6Mn_2O_6$ [30], $K_2Mn_2O_3$ [31], and $KMnO_2$, existing in an inert atmosphere; K_2MnO_4 (decomposes above 550°C [15]); $K_2Mn_4O_9$ (forming at pressures above 50 MPa [33]); and the metastable compounds $K_2Mn_2O_4$ [30] and $K_4Mn_4O_9$ [26] are left out of consideration.

There is particular interest in heterogeneous transformations of K(Rb,Cs)/W/Mn/SiO_2 composite catalysts at typical OCM temperatures. Figure 2b shows the phase diagram of the pseudoquaternary system K_2O–WO_3–Mn_2O_3–SiO_2 at a temperature of 800°C and oxygen pressure of 20 kPa. Under these conditions, there is a melt L, represented by the K_2O–1–2–3–4–5–6–7–8–9 region in the diagram, with two two-phase cavities, 10–11–12–13 (30–78 mol % SiO_2) and 14–15 (30–58 mol % WO_3), because neither K_2SiO_3, nor $K_2Si_2O_5$ [34], nor K_2WO_4 [35, 36] melts at 800°C. Line 11–12 corresponds to the melt

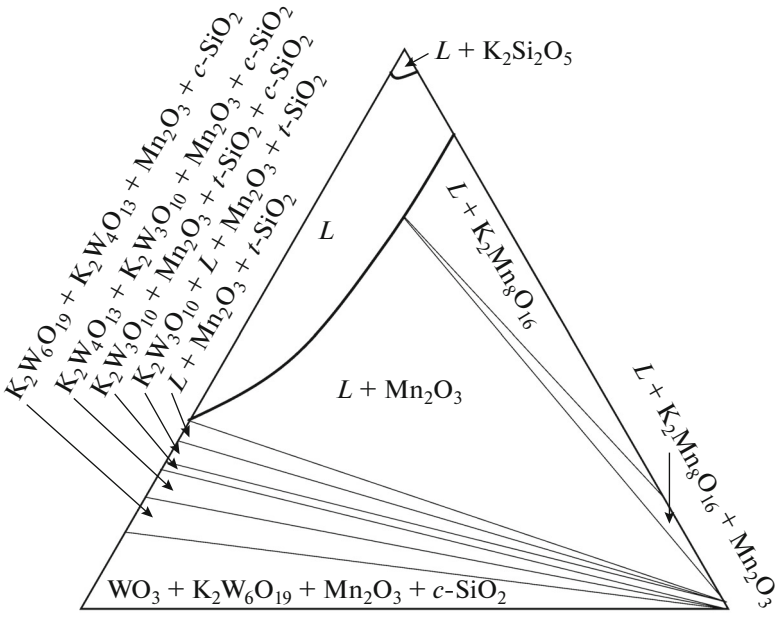

Fig. 3. Section of the isobaric–isothermal phase diagram of the K_2O–WO_3–Mn_2O_3–SiO_2 system ($t = 800$°C, $p_{O_2} = 20$ kPa) at 75 mol % SiO_2.

composition in the three-phase equilibrium K_2S–L–K_2S_2. The melt surface facing Mn_2O_3 includes curves 2–8, 3–7, and 4–6, which correspond to the melt composition in the three-phase equilibria Mn_2O_3–L–K_2M_8, K_2M_8–L–K_2M_4, and K_2M_4–L–K_3M. The curves divide the surface into regions that represent the melt compositions in the two-phase equilibria Mn_2O_3–L (1–2–8–9), K_2M_8–L (2–3–7–8), K_2M_4–L (3–4–7–8), and K_3M–L (4–5–6).

Under these conditions, the stable SiO_2 polymorph is quartz, but because the K_2O–SiO_2 system has a tendency toward the formation of metastable states, which persist for a long time [22, 23], the phase diagram in Fig. 2 includes the actually forming polymorphs: cristobalite (c-SiO_2) and tridymite (t-SiO_2). In a stable state, they coexist in the range 900–1470°C. Between 870 and 900°C, there is tridymite–quartz stable equilibrium [22, 23]. A point of critical importance is the presence of two SiO_2 polymorphs. The melt composition corresponding to tridymite crystallization is represented by curve 1–9.

The SiO_2 content of K/W/Mn/SiO_2 composites usually exceeds 90 mol %, and the corresponding sections are similar to a section of the isobaric–isothermal diagram of the Na_2O–WO_3–Mn_2O_3–SiO_2 system ($t = 800$°C and $p_{O_2} = 20$ kPa) [24], a considerable part of which is the $L + Mn_2O_3 + t$-SiO_2 three-phase field, but sections below 80 mol % SiO_2 will differ markedly. Figure 3 shows a section of the isobaric–isothermal phase diagram of the K_2O–WO_3–Mn_2O_3–SiO_2 system ($t = 800$°C and $p_{O_2} = 20$ kPa) at 75 mol % SiO_2. In addition to the $L + Mn_2O_3$ (melt–bixbyite) region, there is the small region $L + K_2Si_2O_5$ (melt–silicate) and the wide region $L + K_2Mn_8O_{16}$ (melt–cryptomelane), as confirmed by experimental data.

CONCLUSIONS

Analysis of isobaric–isothermal phase diagrams of the K_2O–WO_3–Mn_2O_3–SiO_2 system demonstrates that, in the course of the oxidative coupling of methane, effective K/W/Mn/SiO_2 composite catalysts contain a melt L, which comprises all the components of the catalyst and favors the formation of tridymite (t-SiO_2) on the surface of the cristobalite (c-SiO_2) matrix and the conversion of bixbyite (Mn_2O_3) into nonstoichiometric cryptomelane ($K_{2-x}Mn_8O_{16}$). It seems very likely that such phase transformations take place in the case of Rb/W/Mn/SiO_2 [4, 9–11] and Cs/W/Mn/SiO_2 [4, 8–11] poorly studied composites.

ACKNOWLEDGMENTS

I am grateful to Professor A.S. Loktev (Gubkin Russian State University of Oil and Gas) and Senior Researcher V.A. Artukh (Baikov Institute of Metallurgy and Materials Science, Russian Academy of Sciences) for their assistance in the experimental work.

This study was supported by the Russian Federation Ministry of Education and Science (state research target for the Kurnakov Institute of General and Inorganic Chemistry, Russian Academy of Sciences; basic research).

REFERENCES

1. Li, S., Reaction chemistry of W–Mn/SiO_2 catalyst for the oxidative coupling of methane, *J. Nat. Gas Chem.,* 2003, vol. 12, no. 1, pp. 1–9.
2. Usachev, N.Ya., Kharlamov, V.V., Belanova, E.P., Starostina, T.S., and Krukovskii, I.M., Oxidative processing of light alkanes; state-of-the-art and prospects, *Russ. J. Gen. Chem*., 2009, vol. 79, no. 6, pp. 1251–1263.
3. Erdöhelyi, A., Németh, R., Hancz, A., and Oszkó, A., Partial oxidation of methane on potassium-promoted WO_3/SiO_2 and on K_2WO_4/SiO_2 catalysts, *Appl. Catal., A,* 2001, vol. 211, no. 1, pp. 109–121.
4. Palermo, A., Varquez, J.P.H., and Lambert, R.M., New efficient catalyst for the oxidative coupling of methane, *Catal. Lett.,* 2000, vol. 68, nos. 3–4, pp. 191–196.
5. Lapeña-Rey, N. and Middleton, P.H., The selective oxidation of methane to ethane and ethylene in a solid oxide electrolyte reactor, *Appl. Catal., A,* 2003, vol. 240, nos. 1–2, pp. 207–220.
6. Seimanides, S., Tsiakaras, P., Verykios, X.E., and Vayenas, C.G., Oxidative coupling of methane over yttria-doped zirconia solid electrolyte, *Appl. Catal.,* 1991, vol. 68, no. 1, pp. 41–53.
7. Ji, S., Xiao, T., Li, S., Chou, L., Zhang, B., Xu, C., Hou, R., York, A.P.E., and Green, M.L.H., Surface WO_4 tetrahedron: the essence of the oxidative coupling of methane over M–W–Mn/SiO_2 catalysts, *J. Catal.,* 2003, vol. 220, no. 1, pp. 47–56.
8. Gholipour, Z., Malekzadeh, A., Ghiasi, M., Mortazavi, Y., and Khodadadi, A., Structural flexibility under oxidative coupling of methane; main chemical role of alkali ion in [Mn + (Li, Na, K or Cs) + W]/SiO_2 catalysts, *Iran. J. Sci. Technol.,* 2012, vol. 36, no. A2, pp. 189–211.
9. Nipan, G.D., Dedov, A.G., Loktev, A.S., Ketsko, V.A., Kol'tsova, T.N., Tyunyaev, A.A., and Moiseev, I.I., SiO_2-based composites in the catalysis of methane oxidative coupling: role of phase composition, *Dokl. Phys. Chem.,* 2008, vol. 419, no. 2, pp. 73–76.
10. Tyunyaev, A.A., Nipan, G.D., Kol'tsova, T.N., Loktev, A.S., Ketsko, V.A., Dedov, A.G., and Moiseev, I.I., Polymorphic Mn/W/Na(K,Rb,Cs)/SiO_2 catalysts for oxidative coupling of methane, *Russ. J. Inorg. Chem.,* 2009, vol. 54, no. 5, pp. 664–667.
11. Dedov, A.G., Nipan, G.D., Loktev, A.S., Tyunyaev, A.A., Ketsko, V.A., Parkhomenko, K.V., and Moiseev, I.I., Oxidative coupling of methane: influence of the phase composition of silica-based catalysts, *Appl. Catal., A,* 2011, vol. 406, nos. 1–2, pp. 1–12.
12. Kou, Y., Zhang, B., Niu, J.-Z., Li, S.-B., Wang, H.-Li., Tanaka, T., and Yoshida, S., Amorphous features of working catalysts: XAFS and XPS characterization of Mn/Na_2WO_4/SiO_2 as used for the oxidative coupling of methane, *J. Catal.,* 1998, vol. 173, no. 2, pp. 399–408.
13. Wang, S., Zheng, H., Zhang, Q., Li, Lin., Wu, H., Li, G., and Feng, C., Effects of polyaniline coating of cryptomelane-type KMn_8O_{16} on electrochemical performance for lithium-ion batteries, *J. Nanopart. Res.,* 2014, vol. 16, no. 2, paper 2232.
14. Nipan, G.D., Artukh, V.A., Yusupov, V.S., Loktev, A.S., Spesivtsev, N.A., Dedov, A.G., and Moiseev, I.I., Effect of pressure on the phase composition of Li(Na)/W/Mn/SiO_2 composites and their catalytic activity for oxidative coupling of methane, *Inorg. Mater.,* 2014, vol. 50, no. 9, pp. 912–916.
15. Herbstein, F.H., Ron, G., and Weissman, A., The thermal decomposition of potassium permanganate and related substances. Part I. Chemical aspects, *J. Chem. Soc. A,* 1971, part II, pp. 1821–1826.
16. Liu, Z.-X., Che, M.-W., Baeg, J.-O., and Lee, C.W., Removal of ethylene over $KMnO_4/Al_2O_3$–SiO_2, *Bull. Korean Chem. Soc.,* 2006, vol. 27, no. 12, pp. 2064–2066.
17. Gelsing, R.J.H., Stein, H.N., and Stevels, J.M., The phase diagram K_2WO_4–WO_3, *Rec. Trav. Chim.,* 1965, vol. 84, no. 11, pp. 1452–1458.
18. Zimmerl, T., Schubert, W.-D., Bicherl, A., and Bock, A., Hydrogen reduction of tungsten oxides: alkali additions, their effect on the metal nucleation process and potassium bronzes under equilibrium conditions, *Int. J. Refr. Met. Hard Mater.,* 2017, vol. 62, part B, pp. 87–96.
19. Kazenas, E.K., *Termodinamika ispareniya dvoinykh oksidov* (Thermodynamics of Binary Oxide Vaporization), Moscow: Nauka, 2004.
20. Spitsyn, V.I., Thermal stability and volatility of normal alkali tungstates, *Zh. Obshch. Khim.,* 1950, vol. 20, no. 3, pp. 550–552.
21. Yamdagni, R., Pupp, C., and Porter, R.F., Mass spectrometric study of the evaporation of lithium and sodium molybdates and tungstates, *J. Inorg. Nucl. Chem.,* 1970, vol. 32, no. 11, pp. 3509– 3523.
22. Nipan, G.D., Buzanov, G.A., Zhizhin, K.Yu., and Kuznetsov, N.T., Phase states of Li(Na,K,Rb,Cs)/W/Mn/SiO_2 composite catalysts for oxidative coupling of methane, *Russ. J. Inorg. Chem.,* 2016, vol. 61, no. 14, pp. 1689–1707.
23. Nipan, G.D., Melt-assisted phase transformations of A/W/Mn/SiO_2 (A = Li, Na, K, Rb, Cs) composite catalysts, *Inorg. Mater.,* 2017, vol. 53, no. 6, pp. 553–559.
24. Nipan, G.D., Phase states of Na/W/Mn/SiO_2 composites at temperatures of catalytic oxidative coupling of methane, *Inorg. Mater.,* 2014, vol. 50, no. 10, pp. 1012–1018.
25. Nipan, G.D., Phase states of Li/W/Mn/SiO_2 composites in catalytic oxidative coupling of methane, *Inorg. Mater.,* 2015, vol. 51, no. 4, pp. 389–395.
26. Scholder, R. and Protzer, U., Uber Alkalomanganate(III) bis (V), *Z. Anorg. Allg. Chem.,* 1969, vol. 369, nos. 3–6, pp. 313–326.

27. Delano, P.H., Classification of manganese dioxides, *Ind. Eng. Chem.,* 1950, vol. 42, no. 3, pp. 523–527.

28. De Carvalho, A.J.C., Stages in the preparation of potassium manganate from pyrolusite, *J. Appl. Chem.,* 1957, vol. 7, no. 4, pp. 145–151.

29. Delmas, C. and Fouassier, C., Les phase K_xMnO_2 ($x \leq 1$), *Z. Anorg. Allg. Chem.,* 1976, vol. 420, no. 2, pp. 184–192.

30. Brachtel, G. and Hoppe, R., $K_6[Mn_2O_4]$ und $K_6[Fe_2O_4]$ – ein Verleich, *Z. Anorg. Allg. Chem.,* 1978, vol. 446, no. 1, pp. 64–76.

31. Seipp, E. and Hoppe, R., Ein neues oxomanganat(II): $K_2Mn_2O_3$, *Z. Anorg. Allg. Chem.,* 1985, vol. 530, no. 11, pp. 117–126.

32. Jansen, M., Chang, F.M., and Hoppe, R., Zur Kenntnis von $KMnO_2$, *Z. Anorg. Allg. Chem.,* 1982, vol. 490, no. 1, pp. 101–110.

33. Endo, T., Kume, S., Shimada, M., and Koizumi, M., Synthesis of potassium manganese oxides under hydrothermal conditions, *Mineral. Mag.,* 1974, vol. 39, no. 3, pp. 559–563.

34. Allendorf, M.D. and Spear, K.E., Thermodynamic analysis of silica refractory corrosion in glass-melting furnaces, *J. Electrochem. Soc.,* 2001, vol. 148, no. 2, pp. B59–B67.

35. Chang, L.L.Y. and Sachdev, S., Alkali tungstates: stability relations in the systems $A_2O \cdot WO_3$–WO_3, *J. Am. Ceram. Soc.,* 1975, vol. 58, nos. 7–8, pp. 267–270.

36. Xue, L., Lin, Z., Chen, D., Huang, F., and Liang, J., Subsolidus phase relations in the systems K_2O–ZnO–AO_3 (A = Mo, W), *J. Alloys Compd.,* 2008, vol. 452, no. 2, pp. 263–267.